Regulation of transcription elongation anticipates alternative gene expression strategies across the cell cycle

Douglas Maya-Miles[1,2], José García-Martínez[3], Ildefonso Cases[4], Rocío Pasión[5], Jesús de la Cruz[1,5], José E. Pérez-Ortín[3,*], María de la Cruz Muñoz-Centeno[1,5,*], Sebastián Chávez[1,5,*]

[1]Instituto de Biomedicina de Sevilla, Universidad de Sevilla-CSIC-Hospital Universitario Virgen del Rocío, E41013 Seville, Spain.

[2]Centro de Investigación Biomédica en Red (CIBEREHD), Sevilla, Spain.

[3]Instituto de Biotecnología y Biomedicina (BIOTECMED), Facultad de Biológicas, Universitat de València. E46100 Burjassot, Spain.

[4]Unidad de Bioinformática, Centro Andaluz de Biología del Desarrollo, CSIC-Universidad Pablo de Olavide-Junta de Andalucía, E41013, Seville, Spain.

[5]Departamento de Genética, Facultad de Biología, Universidad de Sevilla, E41012 Seville, Spain.

*Corresponding authors: jose.e.perez@uv.es, mcmunoz@us.es, schavez@us.es

Short title: Regulation of transcription elongation across the cell cycle.

Abstract

A growing body of evidence supports the idea that RNA polymerase II (RNAP II) activity during transcription elongation can be regulated to control transcription rates. Using genomic run-on and RNAP II chromatin immunoprecipitation, we measured both active and total RNAP II across the bodies of genes at three different stages of the mitotic cell cycle in *Saccharomyces cerevisiae*: G1, S, and G2/M. Comparison of active and total RNAP II levels at these stages revealed distinct patterns of transcription elongation control throughout the cell cycle. Previously characterized cycling genes were associated with some of these elongation patterns. A cluster of genes with highly divergent genomic run-on and RNAP II chromatin immunoprecipitation patterns was notably enriched in genes related to ribosome biogenesis and the structural components of the ribosome. We confirmed that the expression of ribosome biogenesis mRNAs increases after G1 but decreases following mitosis. Finally, we analyzed the contribution of mRNA stability to each cluster and found that a coordinated regulation of RNAP II activity and mRNA decay is necessary to fully understand the alternative strategies of gene expression across the cell cycle.

Introduction

44 Phenotypic plasticity in living organisms is driven by the regulation of genome
45 expression. This regulation occurs at all levels of the gene expression pathway, from gene
46 transcription to protein degradation (reviewed in [1]). Transcription is the most highly
47 regulated step in most organisms and under most conditions [2–4], although other steps
48 also play significant roles during physiological dynamic changes [5].
49 Protein-coding gene transcription is carried out by RNA polymerase II (RNAP II), which
50 initiates at gene promoters, elongates pre-mRNAs along gene bodies, and terminates
51 once pre-mRNAs are cleaved and polyadenylated. Historically, most of our
52 understanding of transcriptional regulation has focused on the initiation phase.
53 However, in recent decades, it has become clear that post-initiation regulation is a crucial
54 component of genome expression control [6,7].
55 In higher eukaryotes, transcriptional elongation is primarily regulated through promoter-
56 proximal pausing. In the budding yeast *Saccharomyces cerevisiae*, this mechanism does
57 not occur. However, other forms of elongation regulation are present across the yeast
58 genome [8], which contains all the necessary factors, including chromatin remodeling
59 complexes, histone chaperones, and histone-modifying enzymes, that govern eukaryotic
60 transcription elongation [9,10].
61 During elongation, RNAP II can backtrack on its DNA template, stably blocking mRNA
62 elongation [11]. Backtracked RNAP II requires RNA cleavage to resume transcription [12],
63 a process stimulated by TFIIS [11]. Using RNAP II chromatin immunoprecipitation (RNAp
64 ChIP) and genomic run-on (GRO) assays to compare total and catalytically active
65 elongating polymerases, respectively, we previously demonstrated that certain gene
66 regulons, such as those related to ribosomal proteins, ribosome biogenesis, and

67 mitochondria, are regulated at the elongation level during carbon source changes.
68 Notably, ribosomal protein genes are particularly susceptible to backtracking [8].
69 The *S. cerevisiae* genome undergoes substantial changes in gene expression throughout
70 the cell cycle. Approximately 10% of its mRNAs exhibit cell-cycle periodicity [13]. Some
71 reports suggest this proportion may be as high as 29%, with 37% of the proteome being
72 regulated in a cell-cycle-dependent manner [14], though other studies challenge these
73 findings (reviewed in [15]; see also [16]).
74 In this study, we investigated whether regulation of RNAP II elongation activity plays a
75 role in genome-wide control of gene expression across the cell cycle. Our results show
76 that this regulation is indeed present in a significant portion of the genome. Genes
77 encoding ribosome biogenesis factors appear to be particularly subject to elongation
78 regulation and tend to increase the proportion of active RNAP II molecules just before
79 the onset of mitosis. Furthermore, we found that distinct groups of genes with regulated
80 RNAP II elongation activity also exhibit concomitant control of mRNA stability
81 throughout the cell cycle, suggesting a potential link between these two components of
82 gene regulation.
83

84 # Materials and methods

85

86 **Cell cycle synchronization.**

87

88 BY4741 S. cerevisiae cells, transformed with plasmid pRS316 to become Ura+, were
89 grown to mid-log phase (OD_{600} = 0.25) in minimal complete (SC) medium and

90 synchronized at G1 (START) with 1 μg/ml of alpha factor. At this stage, the percentage
91 of unbudded cells in all three experiments was greater than 90%. The cultures were then
92 washed in fresh media to remove the pheromone and released into new media. Samples
93 for total RNAP II (RNAp ChIP), active RNAP II (GRO), FACS, and microscopy were taken at
94 0, 30, and 60 minutes.
95
96 To determine which cell cycle stage was enriched at each time point, we first performed
97 flow cytometry and budding index analysis. The combination of these two analyses
98 revealed that, at time 0, most cells remained in G1 (unbudded cells with or without
99 shmoo formation and a 1C DNA content), with very few having completed mitosis by 60
100 minutes (indicated by two differentiated nuclear masses). These two analyses are useful
101 for distinguishing the G1 (no bud or shmoo) and mid-late M phase (where the nucleus
102 has started to split) populations, but they are less effective at differentiating between S,
103 G2, and early M phases. Median levels of total and active RNAP II at each time point,
104 based on well-established cell cycle genes [17,18], were used to more accurately infer
105 which cell cycle stages were enriched at each time point analyzed (Fig 1A, C).
106
107 **Genomic Run-On**
108
109 Genomic run-on (GRO) was performed as described in [19] and modified in [20]. Briefly,
110 GRO detects genome-wide, actively elongating RNAP II by macroarray hybridization,
111 with the density of RNAP II per gene used as a measure of its synthesis rate. The protocol
112 also allows for the measurement of mRNA levels for all genes. mRNA half-lives are
113 calculated by dividing the mRNA amount by the synthesis rate, assuming steady-state

114 conditions for the transcriptome. The total synthesis rate was determined by summing
115 the individual gene synthesis rates.
116
117 For the procedure, 5 x 10^8 exponentially growing cells were permeabilized by washing
118 twice with 0.5% N-lauryl sarcosine sodium sulfate (sarkosyl), followed by recovery
119 through low-speed centrifugation. In vivo transcription was then carried out in a solution
120 containing 120 µL of 2.5X transcription buffer (50 mM Tris-HCl, pH 7.7, 500 mM KCl, 80
121 mM MgCl2), 16 µL of AGC mix (10 mM each of CTP, ATP, and GTP), 6 µL of DTT (0.1 M),
122 16 µL of [α33P] UTP (3000 Ci/mmol, 10 µCi/µL), and distilled water up to 300 µL. The
123 mixture was incubated for 5 minutes at 30ºC to facilitate transcription elongation and
124 was subsequently halted by adding 1 mL of cold distilled water. Non-incorporated
125 radioactive nucleotides were removed by two centrifugation wash cycles.
126
127 Total RNA was extracted using the Fast-Prep (Bio101 Inc.) device. Cells were
128 resuspended in 500 µL of LETS buffer (0.1 M LiCl, 10 mM EDTA, 0.2% SDS, 10 mM Tris-
129 HCl, pH 7.4), along with 200 µL of glass beads and 500 µL of water-saturated acid phenol.
130 Contaminants were removed by chloroform extraction, and labeled RNA was
131 precipitated with 0.1 volume of 5 M LiCl and 2.5 volumes of cold ethanol for a minimum
132 of 2 hours at -20ºC. The labeled RNA, obtained after centrifugation and washing, was
133 quantified spectrophotometrically. All in vivo labeled RNA was used for hybridization
134 (0.35–3.5 x 10^7 dpm).
135
136 **Chromatin immunoprecipitation of RNA polymerase II (RNAp ChIP)**
137

138 RNAp ChIP was performed as described in [21]. 5 x 10^8 cells were crosslinked with
139 formaldehyde (FC 1%) for 15 minutes at room temperature. Cross-link was quenched
140 with glycine (FC 125 mM) and washed 4 times with 30 mL ice-cold TBS buffer (20mM
141 Tris-HCl, 140 mM NaCl, pH 7.5) and frozen. Cells were thawed on ice and resuspended
142 in 300 µL lysis buffer [50 mM HEPES-KOH pH 7.5, 140 mM NaCl, 1 mM EDTA, 1% Triton
143 X-100, 0.1% sodium deoxycholate, 1 mM PMSF (Phenylmethylsulfonyl fluoride), 1 mM
144 benzamidine and 1 pill of protease inhibitor cocktail (Roche Diagnostics, Mannheim,
145 Germany) dissolved in every 50 ml of buffer)]. The equivalent of 0.3 ml of frozen glass
146 beads (425-600 mm; Sigma-Aldrich, St Louis, MO, USA) Cell lysis was carried out in a
147 Fast-Prep (Bio101 Inc.) device by 2 cycles of 30 seconds. Samples were cooled down 5
148 minutes in ice between cycles. Samples were then sonicated in ice-cold water using a
149 Bioruptor (Diagenode SA, Liège, Belgium) with 15´ pulses at High output (200W) during
150 2 cycles of 15 minutes. DNA fragments obtained ranged from 200 and 500 bp. Cell debris
151 was removed by centrifugation at 12,000 rpm at 4°C for 5 minutes. An aliquot of 10 µL
152 of this whole cell extract (WCE) was kept as positive control. 50 µL of Dynabeads Protein
153 G (Dynal Invitrogen Corp., Carlsbad, CA, USA) were washed with 5 mg/ml bovine serum
154 albumin (BSA) in PBS buffer (140 mM NaCl, 2.7 mM KCl, 10 mM Na2HPO4, 1.8 mM
155 KH2PO4, pH 7,4) and incubated with anti-Rpb3 antibodies (ab81859; Abcam). Beads
156 were washed with PBS/BSA to remove unbound antibody and incubated for 1.5-2 hours
157 in agitation to enrich the samples in the DNA fragments specifically cross-linked to the
158 RNAP II. Beads were washed twice with lysis buffer, twice with 360 mM NaCl lysis buffer,
159 twice with wash buffer (10 mM Tris-HCl pH 8.0, 250 mM LiCl, 0.5% Nonidet P-40, 0.5%
160 sodium deoxycholate, 1 mM EDTA pH 8.0, 1 mM PMSF, 1 mM benzamidine and 1 pill of
161 protease inhibitor cocktail/25 mL (Roche), and once with TE (10 mM Tris-HCl, pH 8.0, 1

162 mM EDTA). Two successive washes were performed with 30 µL of elution buffer (50 mM
163 Tris-HCl pH 8.0, 10 mM EDTA, 1% SDS) by incubating for 10 minutes at 65°C each time.
164 The final volume of all the samples (IP, NA and WCE) was raised to 300 µL with TE and
165 treated overnight at 65°C to reverse the cross-linking. Proteins were degraded by
166 adding 150 µg of proteinase K for 1h 30 min at 37°C. DNA was purified using QIAquick
167 PCR purification columns (Qiagen Inc., Valencia, CA, USA). Ligation Mediated PCR [3] was
168 used for DNA amplification. Briefly, DNA was blunted by T4 phage DNA polymerase in a
169 reaction volume of 124 µL (T4 DNA Pol buffer, 40 µg/µL BSA, 80 µM dNTPs, 0.6 U T4
170 DNA Polymerase (Roche, Basel, Switzerland). The reaction was allowed to proceed for
171 20 minutes at 12°C. After phenol/chloroform/isoamylic alcohol extraction, DNA was
172 ethanol-precipitated in the presence of 12 µg of glycogen and was ligated in a final
173 volume of 50 µL with the annealed linkers oJW102 and oJW103 (1.5 µM of each primer).
174 The reaction was carried out overnight at 16°C and ligated DNA was precipitated and
175 resuspended in 25 µL milliQ water. The ligated DNA was dissolved in a final volume of
176 40 µL (1x DNA pol buffer: 2 mM MgCl2, 0.25 mM dNTPs, 1.25 µM oligonucleotide
177 oJW102). The reaction was started by incubating for 2 minutes at 55°C, then pausing to
178 add 10 µL of the reaction mix (1x DNA pol buffer, 2 mM MgCl2 and 5 U DNA polymerase
179 from Biotools, Madrid, Spain). The program was resumed for 5 minutes at 72°C, 2
180 minutes at 95°C and 33 cycles of 30 s at 95°C, 30 s at 55°C and 2 minutes at 72°C. DNA
181 was precipitated overnight and resuspended in 50 µL of milliQ water. A 5 µL DNA aliquot
182 of the LM-PCR was analyzed on a 1.2% agarose gel to check the size (average size of 300-
183 400 bp) and PCR efficiency. The PCR product was used as a template for the radioactive
184 labelling reaction. The reaction mixture contained 5-15 µL of amplified DNA in 50 µL (1x
185 DNA pol buffer, 2 mM MgCl2, 0.2 mM dATP, dTTP and dGTP, 25 µM dCTP, 1 µM oJW102,

186 0.8 µCi/µL α-33P-dCTP and 5 U DNA polymerase). The mix was denatured for 5 minutes
187 at 95°C, annealed 5 minutes at 50°C, and amplified for 30 minutes at 72°C. The reaction
188 product was purified through a ProbeQuant G-50 column (Amersham Biosciences,
189 Piscataway, NJ, USA) to remove unincorporated 33P-dCTP and oligonucleotides.
190

191 **Total mRNA extraction**

192

193 Total RNA isolated from budding yeast cells was prepared as described [22], but using a
194 multiple-sample automated device (Fast-Prep®) to break cells.
195

196 **Hybridisation, image analysis and data normalization**

197

198 Nylon filters were made using PCR-amplified whole ORF sequences as probes. After pre-
199 hybridizing nylon membranes for 1 h in 5X SSC, 5X Denhart's, 0.5% SDS, 100 µg/mL
200 salmon sperm DNA, hybridizations were performed using 3-5 mL of the same solution
201 containing labelled RNA. Hybridizations were conducted during 40-44 h in a roller oven
202 at 65°C. After hybridization, filters were washed once in 2X SSC, 0.1% SDS for 30 min,
203 and twice in 0.2X SSC, 0.1% SDS for 30 min. Filters were exposed for up to 7 days to an
204 imaging plate (BAS-MP, FujiFilm) which was read at 50 µm resolution in a
205 phosphorimager scanner (FLA-3000, FujiFilm). Both GRO and RNAp ChIP experiments
206 were performed in triplicate by swapping the filters in each replicate among the
207 different sampling times, as described in [20] Images were quantified by using the
208 ArrayVision 7.0 software (Imaging Research, Inc.). The signal intensity for each spot was
209 the background subtracted ARM Density (Artifact Removed Median). Only those values

210 that were 1.35 times above the corresponding background were taken as valid
211 measurements. To compare the RNAp ChIP data between experiments, the median
212 binding ratio of the 32 rDNA spots were arbitrarily set as background. Reproducibility of
213 the replicates was checked using the ArrayStat software (Imaging Research, Inc.).
214 Normalization between conditions was done using the global median method for RNAp
215 ChIP and for GRO experiments. The ratio between immunoprecipitated (IP) and whole
216 cell extract (WCE) in each experiment (or No-Ab and WCE) after normalization was taken
217 as the binding ratio.
218

219 **Data analyses**

220

221 The changes in RNAp ChIP and GRO data for all genes were evaluated using cluster
222 analysis of log2-transformed and z-score normalized values. The cluster composition
223 was analyzed with WebMeV (Multiple Experiment Viewer) [35], employing the SOTA
224 clustering procedure [23]. Expression data from [17] was averaged across two cycles and
225 z-score normalized. Decay rates from the same source were averaged across samples,
226 log-transformed, and scaled to z-scores. The relationship between GRO and RNAp ChIP
227 was modeled using a linear model without an intercept term. Values for gene categories
228 or cell cycle phases were summarized by the mean, with error bars representing the 95%
229 confidence interval as estimated by 1,000 bootstrap resamples.
230
231

232 # Results

233

234 **Elongating RNA polymerase II is highly dynamic during the cell cycle**

235

236 To determine if the activity of elongating RNAP II undergoes changes throughout the cell
237 cycle, we used alpha-factor to synchronize *S. cerevisiae* populations at START, the
238 decision point within G1 in which cells commit to a new round of cell division [24]. We
239 then released cells from the arrest and took samples for total RNAP II (ChIP) or active
240 RNAP II (Genomic run-on) at 0, 30 and 60 minutes (see scheme in Fig 1A). FACS profile
241 and budding index were used to estimate the average cell cycle stage of each sample
242 (S1 Fig). Almost all cells from samples at time 0 were in G1, whereas most cells in the 60
243 min samples were in G2/M. Cells from the 30 min samples were in between, with at
244 least one third of them exhibiting the characteristic small bud of S phase, indicating a
245 clear enrichment in this phase.

246

247 **Figure 1: Distribution of Total and Active RNA Polymerase II at Genes During the**
248 **Transition from G1 to G2.** A) Schematic representation of the time points and samples
249 taken for the analysis of total and active RNAP II. B) Plot representing total (RNAp ChIP)
250 and active RNAP II (GRO) present at each gene at each time point analyzed. Black line:
251 Overall tendency. Dashed blue line: Cycling genes. C) Behavior of total (RNAp ChIP) and
252 active RNAP II (GRO) of cyclically expressed genes, classified according to the phase of
253 maximal expression (G1, G1/S, S, S/G2, G2/M, and M) using CycleBase 3.0 as a reference
254 (S1 Table). Total mRNA expression and mRNA decay values from Eser et al. [17] are also
255 shown.

256

257 First analyses revealed many genes in which the levels of active and total RNAP II change
258 during the cell cycle (S2A Fig). As shown in Fig 1B, global correlation between total RNAP
259 II (ChIP) and active RNAP II (GRO) was significant and oscillated across the cell cycle,
260 showing a maximum Pearson correlation coefficient (R^2) of 0.41 at the 30 min timepoint
261 after START. When we focused in the subset of genes with significant periodic regulation
262 across the cell cycle [18], correlation between total and active RNAP II was slightly higher
263 in G1 (R^2 value of 0.38 versus 0.31 in all genes) and in S-G2 (R^2 value of 0.44 versus 0.41)
264 (Fig 1B).
265 We analyzed RNAP II behavior in the different categories of cyclic genes, according to its
266 phase of maximal expression (S1 Table). We found rather parallel RNAP II ChIP and GRO
267 average profiles (Fig 1C). Using the previously published data from Cramer's lab [17], we
268 also found that these transcriptional patterns were similar to their corresponding mRNA
269 profiles, and symmetrical to those of mRNA decay (Fig 1C, see later).
270 This parallelism between total and active RNAP II patterns in cyclic genes supports the
271 technical consistency of our experimental data. However, some subtle differences
272 between the RNAP II ChIP and GRO average profiles were detected, particularly in the
273 G1-S and M genes (Fig 1C). Moreover, the modest global correlation of RNAP II ChIP and
274 GRO across the genome (Fig 1B) seemed to indicate that the control of elongation
275 dynamics might contribute to cell cycle regulation. We hypothesized that changes in
276 gene expression during the cell cycle may result from a variety of strategies in which
277 transcription would be regulated, not only by increasing or decreasing the number of
278 RNAP II molecules engaged on a gene, but also by changing their catalytic activity during
279 elongation.
280

281

282 **Some cycling genes are transcriptionally regulated at the elongation step**

283

284 To uncover these putative regulatory strategies, we clustered all genes according to their
285 RNAP II ChIP and GRO profiles along the cell cycle. We followed the SOTA procedure [23],
286 using the linear correlation coefficient as the distance metric between genes and a
287 variability threshold of 40% as training conditions (S2B Fig). This resulted in ten distinct
288 clusters, named A to J, which divided the gene set into consistent groups (Fig 2A, S1
289 Table). Average GRO and RNAP II ChIP signals for each cluster are shown in Fig 2B,
290 alongside mRNA expression and decay data from [17] (see later).

291

292 **Figure 2: Clustering analysis of total and active RNAP II at genes during the transition**
293 **from G1 to G2.** A) Overview of the different clusters identified through SOTA analysis.
294 B) Behavior of total RNAP II (RNAp ChIP) and active RNAP II (GRO) in each identified
295 cluster. mRNA expression and mRNA decay data from Eser et al. [17] are also presented.
296 Genes included in each cluster, along with all transcriptomic data, are listed in S1 Table.
297 To determine the proportion of active polymerases, we performed a linear regression
298 analysis using GRO as the dependent variable and RNAp ChIP as the predictor, without
299 an intercept term. The resulting regression coefficient represents the fraction of RNA
300 polymerases actively engaged in transcription. By interpreting this coefficient as the
301 efficiency of polymerase engagement, we estimate the percentage of active
302 polymerases relative to the total chromatin-bound population. C) Distribution of cell
303 cycle genes according to their peak of maximal expression (CellCycleBase 3.0) [18] in
304 each of the clusters identified. Green arrows indicate groups in which the enrichment

305 or depletion of cell cycle genes is statistically significant (logistic regression with
306 Benjamini-Hochberg correction). D) Transcription factors known to regulate genes
307 belonging to the clusters described in A. Only transcription factors significantly enriched
308 in one or two clusters (Yeastrack [25], hypergeometric test $p < 10^{-5}$), according to DNA
309 binding or expression evidence, are shown. Other transcription factors significantly
310 enriched in three or more clusters include: Bas1, Cst6, Tec1, Gat1, Cbf1, Met28, Pdr1,
311 Gcn4, Met31, Met32, Pdr3, Rpn4, and Yap1.
312
313 Some clusters exhibited parallel profiles for total (ChIP) and active RNAP II (GRO). For
314 instance, cluster C showed significant decreases in both RNAP II ChIP and GRO signals at
315 the 30-minute time point, followed by a minimal change at 60 minutes (Fig 2B). A
316 similarly simple regulation was observed in cluster G, which displayed a sustained
317 increase in both RNAP II ChIP and GRO signals after G1 (Fig 2B). Finally, cluster J exhibited
318 peaks of both RNAP II ChIP and GRO at the 30-minute time point (Fig 2B). In all three of
319 these clusters, regulation is likely exerted by controlling RNAP II recruitment, with little
320 or no modulation of its elongation activity.
321 In contrast, the other seven clusters exhibited different patterns of average RNAP II ChIP
322 and GRO signals, with some of them showing completely dissimilar profiles (Fig 2B). For
323 example, cluster B displayed a marked decrease in RNAP II ChIP at 60 minutes after G1,
324 while showing a peak in GRO at 30 minutes (Fig 2B). Cluster H showed increased RNAP
325 II ChIP signals at both 30 and 60 minutes, but a flat pattern in GRO (Fig 2B). The opposite
326 was observed in cluster F, where RNAP II ChIP signals increased slightly at 30 minutes,
327 whereas GRO signals dropped at this time point and remained low at 60 minutes (Fig
328 2B). Cluster A also exhibited a distinct pattern: a flat RNAP II ChIP profile with a strong

329 increase in GRO after G1, peaking at the 30-minute time point (Fig 2B). Unparallel
330 profiles were also observed in clusters D and I, where RNAP II ChIP signals decreased and
331 increased, respectively, 30 minutes after G1, without comparable changes in their GRO
332 profiles (Fig 2B).

333 We next examined whether these alternative patterns of RNAP II elongation were
334 significant for the expression of cycling genes in the ten clusters, as defined by Cyclebase
335 [18]. We found significant enrichment, either positive or negative, in most clusters.
336 Positive enrichments were particularly clear in clusters D and E (G1 genes), G (M genes),
337 I (S/G2 and G2/M genes), and J (S, S/G2, and G2/M genes) (Fig 2C). Additionally, when
338 we examined the presence of our clusters within previously defined cycling gene
339 subgroups, we found significant enrichment of clusters D, E, and F in G1 genes, and of
340 cluster G in M genes (S3 Fig). Interestingly, we also observed significant exclusion of all
341 clusters except B, G, I, and J from G2/M genes (S3 Fig). Furthermore, clusters D, E, and F
342 were significantly excluded from S/G2 genes (S3 Fig).

343 Notably, some clusters displaying dissimilar RNAP II ChIP and GRO profiles across the cell
344 cycle, such as D, F and I, were associated with cycling genes in the analyses mentioned
345 above. GRO and RNAp ChIP profiles of several G1-expressed genes belonging to cluster
346 D are shown in S4A Fig. Examples of G1- and G1/S-expressed genes from cluster F, and
347 S/G2- and G2/M genes from cluster I are also shown (S4B-C Fig). These results suggest
348 that regulation of RNAP II activity during transcription elongation is compatible with cell
349 cycle control of gene expression, establishing a link between transcription elongation
350 dynamics and cell cycle regulation.

351 We also investigated whether the genes within each cluster shared specific
352 transcriptional activators or repressors, based on previous experimental evidence. We

353 used the "Rank by TF" tool from the Yeastrack database [25]. We found that most clusters
354 were significantly enriched in genes regulated by specific activators or repressors (Fig
355 2D). For instance, cluster G was enriched in genes regulated by Spt10, Spt2, and Hif1, all
356 of which are known to control histone gene transcription in S phase [26], as well as by
357 Thi2, an activator of thiamine pyrophosphate biosynthesis genes, which are upregulated
358 during mitosis [16] (Fig 2D).
359

360 **Regulation of RNA polymerase II elongation explains the cycling pattern**
361 **of ribosome biogenesis genes.**

362

363 We wondered whether the genes in each cluster, in addition to sharing common
364 transcriptional regulation, also exhibited functional similarities. Gene ontology (GO)
365 analysis confirmed that this was indeed the case (S2 Table).
366 For example, cluster A was enriched in terms related to ribosome biogenesis and the
367 structural constituents of ribosomes (ribosomal proteins) (Fig 3A). These categories
368 correspond to the so-called “RiBi” and “RP” regulons, respectively [17]. Consistent with
369 these findings, we observed that cluster A genes were enriched in the global activator
370 Gcr1, known to act as a coactivator of Rap1 in the regulation of ribosomal protein genes
371 [27] (Fig 2D). A significant proportion of cluster A genes also appeared to be targets of
372 Sfp1 and Rph1 (Fig 2D). These two regulators mediate the control of ribosomal protein
373 genes in response to nutrient and stress signaling [28,29], and their molecular functions
374 are connected to transcription elongation. Sfp1 promotes RNA pol II backtracking in its
375 target genes [30,31], while Rph1, a histone H3-K36 demethylase, is linked to chromatin
376 dynamics in the context of RNAP II elongation [32].

377

378 **Figure 3: Cell cycle and functional analysis of total and active RNAP II across the cell**
379 **cycle.** A) Gene ontology analysis with gProfiler for genes in cluster A. B) Similar analysis
380 for genes in cluster D. C) Distribution of identified clusters and logistic regression
381 analyses within the RIBI regulon and subcategories (upper section) and within the RP
382 regulon and subcategories (lower section). D) Representation of total RNAP II (RNAp
383 ChIP) and active RNAP II (GRO) in RiBi and RP genes. mRNA expression and mRNA decay
384 data from Eser et al. [17] are also represented. E) Normalized values for all genes (grey),
385 RiBi regulon (red), and RP regulon (green) for total RNAP II (RNAp ChIP) and active RNA
386 Pol II (GRO). The proportion of active polymerases was calculated as described in Figure
387 1B.

388

389 Cluster D was enriched in a wide set of categories related to respiration and metabolic
390 pathways localized to mitochondria (Fig 3B). Interestingly, genes in cluster D were also
391 enriched in specific targets of Sfp1 and Rph1 (Fig 2D).
392 Given the high significance of their GO categories, we focused on cluster A and the
393 ribosome biogenesis genes, whose regulation is critical for cell growth (reviewed in [33];
394 see also [34]). We analyzed the cluster distribution of the 207 genes from the RiBi
395 regulon present in our dataset and found that more than 50% belonged to cluster A,
396 confirming the significance of this enrichment. In contrast, most other clusters were
397 either not enriched or significantly depleted of this regulon (Fig 3C). All RiBi regulon
398 subgroups, including genes involved in nucleotide metabolism, translation factors, and
399 tRNA synthetases, were highly represented in cluster A (Fig 3C).

400 We also examined the average GRO and RNAp ChIP profiles of the entire RiBi regulon.
401 As in cluster A, between the 0 and 30-minute time points, the GRO signal increased more
402 than the RNAp ChIP signal (Fig 3D). For the RP regulon, less dissimilar average profiles of
403 total and active RNAP II were observed (Fig 3D). This difference from the cluster A
404 average can be explained by the fact that ribosomal protein genes were not only
405 enriched in cluster A but also in cluster G (Fig 3C), which shows a similar GRO profile to
406 cluster A but with a parallel RNAp ChIP profile (Fig 2B). Ribosomal protein genes in
407 cluster G mainly encode components of the large ribosomal subunit (Fig 3C). The
408 significance of this finding is unclear, but it may reflect the existence of different
409 regulatory mechanisms for the synthesis of each ribosomal subunit.
410 Moreover, the differences between the RP and RiBi regulons are consistent with the
411 overall correlation between GRO and RNAp ChIP signals for these gene groups across the
412 cell cycle. While ribosomal protein genes exhibited very high R^2 values at all three time
413 points (between 0.89 and 0.94), RiBi genes showed a drastic increase in correlation from
414 0 ($R^2 = 0.40$) to 30 minutes ($R^2 = 0.70$) (Fig 3E).
415 Ribosome-related mRNAs have not been systematically described as undergoing cyclic
416 regulation [18], although a recent study supports the periodic regulation of genes
417 related to rRNA synthesis, cytoplasmic translation, and ribosome biogenesis at the
418 proteomic level [14]. We analyzed mRNA expression of a subset of eight genes from the
419 RiBi and RP regulons by RT-PCR in alpha factor-synchronized cells. All analyzed RiBi genes
420 exhibited peaks of expression 20 minutes after release from alpha factor (S5 Fig). This
421 cycling pattern was not as clear in the three ribosomal protein genes analyzed (S5 Fig).
422 We conclude that most genes of the RiBi regulon control their expression across the cell
423 cycle by altering RNAP II activity during transcription elongation.

424

425 **RNA polymerase II elongation patterns define alternative gene expression**

426 **strategies during the cell cycle**

427

428 The RiBi regulon is a good example where GRO profiles anticipated mRNA expression
429 patterns better than RNAP II ChIP (Fig 3D). To extend this perspective, we represented
430 the average mRNA levels of these clusters, using the accurate transcriptomic
431 quantification of synchronized cells after START performed by Eser et al. [17]. We
432 confirmed that, in most cases, mRNA expression profiles followed GRO values more
433 closely than RNAP II ChIP (compare the RNAP II ChIP, GRO, and mRNA expression panels
434 in Fig 2B).

435 However, two clear exceptions were detected. Clusters D and I, which are enriched in
436 G1-expressed genes and S/G2/M genes, respectively (Fig 2C), showed a closer
437 parallelism of mRNA expression profiles to RNAP II ChIP than to GRO (Fig 2B). These two
438 cases were puzzling, since RNAP II activity measured by GRO should be a better proxy
439 for transcription than total RNAP II present on genes, as the latter includes both
440 backtracked RNAP II molecules and actively elongating ones [8,31,35,36].

441 To understand these cases, we incorporated mRNA decay values along the cell cycle,
442 which were obtained by Cramer's laboratory [17] using a metabolic labeling approach.
443 As previously described, this additional information aids in understanding the regulatory
444 behavior of cycling genes. For example, the decrease in mRNA expression of G1/S genes
445 at the 30-minute time point is better explained by increased mRNA decay than by the
446 relatively flat profile of transcriptional activity measured by GRO (Fig 1C).

447 This additional layer of information allowed us to explain the divergence between GRO
448 and mRNA expression profiles detected in clusters D and I. We found that average mRNA
449 decay values in cluster D were maximal at 30 minutes (Fig 2B). Therefore, the
450 combination of a mild decrease in transcriptional activity (GRO) with a marked increase
451 in mRNA decay explains the strong downregulation of mRNA expression levels for this
452 group of genes at the 30-minute time point (Fig 2B).
453 In contrast, cluster I showed a mild increase in transcriptional activity (GRO) combined
454 with a slight decrease in mRNA decay, which explains the comparatively higher increase
455 in mRNA expression at 30 minutes (Fig 2B). In fact, comparing clusters I and J, which
456 showed nearly identical mRNA expression profiles, is illustrative of two alternative
457 strategies that result in the same average mRNA expression pattern. In cluster I, mRNA
458 expression regulation is achieved by comparable changes in RNAP II activity and mRNA
459 decay, whereas in cluster J, regulation of RNAP II activity was much more pronounced
460 (Fig 2B). This difference is likely due to the overall higher stability (lower decay) of mRNAs
461 in cluster J compared to cluster I (Fig 2B). As expected, transcriptional regulation of
462 stable mRNAs involves more intense changes in transcriptional activity than for unstable
463 mRNAs. GRO changes also triggered stronger alterations of mRNA expression in
464 ribosome biogenesis genes than in ribosomal protein genes, which exhibited much more
465 stable mRNAs (Fig 3D).
466 The comparison of clusters D and E is also very informative. These two sets of genes
467 shared similar overall mRNA stabilities, intermediate between those of clusters I and J
468 (Fig 2B). In this context, the stronger regulation of transcriptional activity shown by
469 cluster E was insufficient to match the regulatory effect in mRNA levels observed in

470 cluster D, which combined milder control of transcription activity with a more
471 pronounced change in mRNA stability (Fig 2B).
472 A similar conclusion was reached when comparing clusters A (stable mRNAs) and H (very
473 unstable mRNAs). In this case, drastic upregulation of transcriptional activity with no
474 regulation of mRNA decay (cluster A) produced the same average mRNA expression
475 pattern as no change in transcriptional activity combined with slight downregulation of
476 decay (cluster H).
477 The synergistic effect produced by the combined control of transcription and decay was
478 also evident when we compared clusters A and G, both of which express stable mRNAs.
479 These two clusters exhibited upregulated GRO profiles after START; however, in the case
480 of cluster G, its combination with mRNA decay downregulation led to stronger
481 upregulation of mRNA levels than in cluster A, where no significant change in decay was
482 detected (Fig 2B). Thus, in all ranges of mRNA stability, the most pronounced regulation
483 of mRNA levels was achieved by concerted control of RNAP II activity and mRNA decay.
484
485

486 # Discussion

487

488 The comparison of total RNAP II occupancy on gene bodies, as measured by ChIP (RNAP
489 II ChIP), with transcriptional activity assessed by genomic run-on (GRO) allowed us to
490 test whether the regulation of transcription elongation plays a significant role in gene
491 expression across the cell cycle. Only 21% of the 4,764 analyzed genes were classified
492 into clusters that exhibited parallel RNAp ChIP and GRO profiles after alpha factor

493 release (Fig 2B and S2 Fig), indicating that most budding yeast genes undergo some form
494 of regulation at the RNAP II activity level.
495 Several gene clusters were significantly enriched in genes previously shown to exhibit a
496 cyclic pattern of mRNA expression. This was the case for cluster G, which is associated
497 with M-specific genes and their transcription regulators (Fig 2C-D), and which displayed
498 parallel RNAp ChIP, GRO, and mRNA expression profiles (Fig 2B). No alterations in
499 transcriptional activity during elongation are required to explain the regulatory behavior
500 of these genes.
501 In contrast, clusters D (enriched in G1-specific genes) and I (enriched in S-G2-M genes)
502 displayed dissimilar RNAp ChIP and GRO profiles (Fig 2B, S4 Fig), indicating that some
503 alterations in RNAP II activity must occur during transcription elongation, likely through
504 RNAP II backtracking. In these two cases, GRO profiles alone did not explain the mRNA
505 expression patterns, unless mRNA decay was also considered (Fig 2B, see later).
506 Interestingly, cluster A, which also exhibited non-parallel RNAp ChIP and GRO average
507 profiles, contained more than 50% of the RiBi regulon (Fig 3A). Although these genes
508 were not previously described as periodic [18], we confirmed this regulation for some
509 examples through RT-PCR (S5 Fig) and found a regulated mRNA expression pattern for
510 the entire ribosome biogenesis group in the cell-cycle expression dataset produced by
511 Eser et al. [17] (Fig 3D).
512 RNAP II activity in ribosomal protein and ribosome biogenesis genes has previously been
513 shown to be regulated during elongation in response to environmental stimuli mediated
514 by protein kinase A [8]. Interestingly, another regulon capable of modulating its
515 elongating RNAP II activity in response to these conditions is composed of genes related

516 to respiration and other mitochondrial functions [8]. GO analyses revealed significant
517 enrichment of this type of genes in cluster D (Fig 3B).
518 We have previously described that these regulons change their expression in response
519 to cell growth in opposite directions: mRNA concentrations of ribosomal protein and
520 ribosome biogenesis genes increase with the growth rate, whereas mRNA
521 concentrations of mitochondria-related genes decrease, in line with the low respiratory
522 activity of fast-growing yeast cultures [37]. These controls occur through different
523 mechanisms: ribosomal protein and ribosome biogenesis genes upregulate
524 transcription with cell growth without overall changes in mRNA stability, while
525 mitochondria-related genes decrease mRNA stability with increasing growth rate,
526 without significant alterations in transcription rates [37,38]. In agreement with this, the
527 regulation of mRNA levels in cluster A, and more specifically in ribosome biogenesis and
528 ribosomal protein genes, appears to be primarily transcriptional (Figs 2B and 3E),
529 whereas the mRNA expression in cluster D across the cell cycle requires mRNA decay to
530 be considered (Fig 2B).
531 The decreased expression of mitochondria-related genes at the 30-minute time point,
532 when at least one third of the cells were in S phase, aligns with published evidence
533 suggesting that DNA replication occurs during the reductive phase of the *S. cerevisiae*
534 metabolic cycle [39,40]. The increased expression of ribosome biogenesis genes at this
535 time point is likely related to the S-phase, as nucleolus biogenesis is coupled with rDNA
536 replication [41]. Moreover, the synthesis of a complete set of new RNA polymerase I
537 and ribosome components, particularly biogenesis factors, is required before the
538 complete nucleolar reorganization that occurs in mitosis [42].

539 As discussed earlier, D and I are the two clusters where: i) alterations in RNAP II activity,
540 likely due to backtracking, are occurring, and ii) mRNA stability is playing a significant
541 role in regulation. The fact that genes clustered according to elongating RNAP II activity
542 features (RNAp ChIP/GRO profiles) show distinct mRNA decay profiles underscores the
543 importance of transcriptional elongation dynamics in gene expression across the cell
544 cycle. This was especially evident when comparing clusters I and J, which display
545 identical average mRNA expression profiles but differ in mRNA stabilities (Figs 2B).
546 A molecular connection between RNAP II elongation dynamics and the stability of
547 transcribed mRNA was recently described by us for genes controlled by the transcription
548 factor Sfp1 [30]. During transcription of these genes, Sfp1 promotes RNAP II
549 backtracking until late elongation, when it is transferred from the polymerase to the
550 nascent mRNA, which then becomes imprinted for higher stability [30]. It is tempting to
551 hypothesize that a similar mechanism could be operating in the genes of clusters D and
552 I. In fact, genes in cluster D are significantly enriched in targets of Sfp1 (Fig 2D). In this
553 regard, the mRNA stability of mitochondria-related genes (enriched in cluster D, Fig 2B)
554 is controlled by Puf3, a factor that has been proposed to bind its targets co-
555 transcriptionally [43].
556 In addition to Puf3-regulated ones, other genes whose mRNAs are targeted by RNA
557 binding proteins that control their stability also exhibit transcriptional
558 activation/repression, indicating the existence of specific mechanisms of crosstalk,
559 which sum up effects on synthesis and decay rates as a way to enhance regulation [44].
560 These mechanisms of crosstalk may involve complex interactions between
561 transcriptional regulators and RNA-binding proteins that are dynamically modulated
562 across the cell cycle. Such interactions not only influence gene expression but also fine-

563 tune the stability of the mRNA transcripts, contributing to the precise regulation
564 required for cellular processes such as growth and division. Indeed, the balance between
565 transcriptional activity and mRNA decay is crucial for maintaining the appropriate levels
566 of gene products at different stages of the cell cycle.
567

568 # Acknowledgements

569 We thank all members of the IBiS Gene Expression and Ribosome Biogenesis Labs for
570 their helpful scientific discussions, and all technicians from the IBiS and CITIUS facilities
571 for their experimental assistance.
572
573

574 # References

575 1. Pérez-Ortín JE, Tordera V, Chávez S. Homeostasis in the Central Dogma of
576 molecular biology: the importance of mRNA instability. RNA Biol. 2024;16:
577 1659–1666. doi:10.1080/15476286.2019.1655352
578 2. Li JJ, Biggin MD. Statistics requantitates the central dogma. Science (1979).
579 2015;347: 1066–1067. doi:10.1126/science.aaa8332
580 3. Battle A, Khan Z, Wang SH, Mitrano A, Ford MJ, Pritchard JK, et al. Impact of
581 regulatory variation from RNA to protein. Science (1979). 2015;347: 664–667.
582 doi:10.1126/science.1260793
583 4. Jovanovic M, Rooney MS, Mertins P, Przybylski D, Chevrier N, Satija R, et al.
584 Dynamic profiling of the protein life cycle in response to pathogens. Science
585 (1979). 2015;347. doi:10.1126/science.1259038
586 5. Martin B, Suter DM. Gene expression flux analysis reveals specific regulatory
587 modalities of gene expression. iScience. 2023;26: 107758.
588 doi:10.1016/j.isci.2023.107758
589 6. Aoi Y, Shilatifard A. Transcriptional elongation control in developmental gene
590 expression, aging, and disease. Mol Cell. 2023;83: 3972–3999.
591 doi:10.1016/j.molcel.2023.10.004
592 7. Sun R, Fisher RP. The CDK9-SPT5 Axis in Control of Transcription Elongation by
593 RNAPII. J Mol Biol. 2025;437: 168746. doi:10.1016/j.jmb.2024.168746
594 8. Pelechano V, Jimeno-González S, Rodríguez-Gil A, García-Martínez J, Pérez-Ortín
595 JE, Chávez S. Regulon-specific control of transcription elongation across the

596 yeast genome. PLoS Genet. 2009;5: e1000614.
597 doi:10.1371/journal.pgen.1000614
598 9. Farnung L. Chromatin Transcription Elongation – A Structural Perspective. J Mol
599 Biol. 2025;437: 168845. doi:10.1016/J.JMB.2024.168845
600 10. Chen Y, Cramer P. RNA polymerase II elongation factors use conserved
601 regulatory mechanisms. Curr Opin Struct Biol. 2024;84: 102766.
602 doi:10.1016/J.SBI.2023.102766
603 11. Cheung ACM, Cramer P. Structural basis of RNA polymerase II backtracking,
604 arrest and reactivation. Nature. 2011;471. doi:10.1038/nature09785
605 12. Sigurdsson S, Dirac-Svejstrup AB, Svejstrup JQ. Evidence that Transcript
606 Cleavage Is Essential for RNA Polymerase II Transcription and Cell Viability. Mol
607 Cell. 2010;38. doi:10.1016/j.molcel.2010.02.026
608 13. Bähler J. Cell-cycle control of gene expression in budding and fission yeast.
609 Annual Review of Genetics. 2005.
610 doi:10.1146/annurev.genet.39.110304.095808
611 14. Campbell K, Westholm J, Kasvandik S, Di Bartolomeo F, Mormino M, Nielsen J.
612 Building blocks are synthesized on demand during the yeast cell cycle. Proc Natl
613 Acad Sci U S A. 2020;117: 7575–7583. doi:10.1073/pnas.1919535117
614 15. No E-G, Blank HM, Polymenis M. Patterns of protein synthesis in the budding
615 yeast cell cycle: variable or constant? Microbial Cell. 2024;11: 321–327.
616 doi:10.15698/mic2024.08.835
617 16. Blank HM, Papoulas O, Maitra N, Garge R, Kennedy BK, Schilling B, et al.
618 Abundances of transcripts, proteins, and metabolites in the cell cycle of budding
619 yeast reveal coordinate control of lipid metabolism. Mol Biol Cell. 2020;31.
620 doi:10.1091/MBC.E19-12-0708
621 17. Eser P, Demel C, Maier KC, Schwalb B, Pirkl N, Martin DE, et al. Periodic mRNA
622 synthesis and degradation co-operate during cell cycle gene expression . Mol
623 Syst Biol. 2014;10: 717. doi:10.1002/msb.20140001
624 18. Santos A, Wernersson R, Jensen LJ. Cyclebase 3.0: A multi-organism database on
625 cell-cycle regulation and phenotypes. Nucleic Acids Res. 2015;43: D1140–D1144.
626 doi:10.1093/nar/gku1092
627 19. García-Martínez J, Aranda A, Pérez-Ortín JE. Genomic Run-On Evaluates
628 Transcription Rates for All Yeast Genes and Identifies Gene Regulatory
629 Mechanisms. Mol Cell. 2004;15: 303–313. doi:10.1016/j.molcel.2004.06.004
630 20. Oliete-Calvo P, Serrano-Quílez J, Nuño-Cabanes C, Pérez-Martínez ME, Soares
631 LM, Dichtl B, et al. A role for Mog1 in H2Bub1 and H3K4me3 regulation affecting
632 RNAPII transcription and mRNA export. EMBO Rep. 2018;19.
633 doi:10.15252/embr.201845992
634 21. García-Martínez J, Pelechano V, Pérez-Ortín JE. Genomic-Wide Methods to
635 Evaluate Transcription Rates in Yeast. 2011. pp. 25–44. doi:10.1007/978-1-
636 61779-086-7_2
637 22. Sherman F, Fink G, Hicks J. Methods in Yeast Genetics: A Laboratory Course
638 Manual. Cold Spring Harbor Laboratory Press; 1987. Available:
639 https://books.google.es/books?id=lQMmAAAACAAJ
640 23. Herrero J, Valencia A, Dopazo J. A hierarchical unsupervised growing neural
641 network for clustering gene expression patterns. Bioinformatics. 2001;17: 126–
642 136. doi:10.1093/bioinformatics/17.2.126

643 24. Hartwell LH, Culotti J, Pringle JR, Reid BJ. Genetic control of the cell division
644 cycle in yeast. Science. 1974. doi:10.1126/science.183.4120.46
645 25. Teixeira MC, Viana R, Palma M, Oliveira J, Galocha M, Mota MN, et al.
646 YEASTRACT+: a portal for the exploitation of global transcription regulation and
647 metabolic model data in yeast biotechnology and pathogenesis. Nucleic Acids
648 Res. 2023;51: D785–D791. doi:10.1093/nar/gkac1041
649 26. Dannah NS, Nabeel-Shah S, Kurat CF, Sabatinos SA, Fillingham J. Functional
650 Analysis of Hif1 Histone Chaperone in *Saccharomyces cerevisiae*. G3
651 Genes|Genomes|Genetics. 2018;8: 1993–2006. doi:10.1534/g3.118.200229
652 27. Willis KA, Barbara KE, Menon BB, Moffat J, Andrews B, Santangelo GM. The
653 Global Transcriptional Activator of *Saccharomyces cerevisiae* , Gcr1p, Mediates
654 the Response to Glucose by Stimulating Protein Synthesis and *CLN* -Dependent
655 Cell Cycle Progression. Genetics. 2003;165: 1017–1029.
656 doi:10.1093/genetics/165.3.1017
657 28. Shu W-J, Chen R, Yin Z-H, Li F, Zhang H, Du H-N. Rph1 coordinates transcription
658 of ribosomal protein genes and ribosomal RNAs to control cell growth under
659 nutrient stress conditions. Nucleic Acids Res. 2020;48: 8360–8373.
660 doi:10.1093/nar/gkaa558
661 29. Marion RM, Regev A, Segal E, Barash Y, Koller D, Friedman N, et al. Sfp1 is a
662 stress- and nutrient-sensitive regulator of ribosomal protein gene expression.
663 Proceedings of the National Academy of Sciences. 2004;101: 14315–14322.
664 doi:10.1073/pnas.0405353101
665 30. Kelbert M, Jordán-Pla A, de Miguel-Jiménez L, García-Martínez J, Selitrennik M,
666 Guterman A, et al. The zinc-finger transcription factor Sfp1 imprints specific
667 classes of mRNAs and links their synthesis to cytoplasmic decay. VijayRaghavan
668 K, editor. Elife. 2024;12: RP90766. doi:10.7554/eLife.90766
669 31. Gómez-Herreros F, de Miguel-Jiménez L, Morillo-Huesca M, Delgado-Ramos L,
670 Muñoz-Centeno MC, Chávez S. TFIIS is required for the balanced expression of
671 the genes encoding ribosomal components under transcriptional stress. Nucleic
672 Acids Res. 2012;40: 6508–6519. doi:10.1093/nar/gks340
673 32. Kim T, Buratowski S. Two Saccharomyces cerevisiae JmjC Domain Proteins
674 Demethylate Histone H3 Lys36 in Transcribed Regions to Promote Elongation.
675 Journal of Biological Chemistry. 2007;282: 20827–20835.
676 doi:10.1074/jbc.M703034200
677 33. de la Cruz J, Gómez-Herreros F, Rodríguez-Galán O, Begley V, de la Cruz Muñoz-
678 Centeno M, Chávez S. Feedback regulation of ribosome assembly. Curr Genet.
679 2018;64: 393–404. doi:10.1007/s00294-017-0764-x
680 34. Gómez-Herreros F, Margaritis T, Rodríguez-Galán O, Pelechano V, Begley V,
681 Millán-Zambrano G, et al. The ribosome assembly gene network is controlled by
682 the feedback regulation of transcription elongation. Nucleic Acids Res. 2017;45:
683 9302–9318. doi:10.1093/nar/gkx529
684 35. Rodríguez-Gil A, García-Martínez J, Pelechano V, Muñoz-Centeno M de la C, Geli
685 V, Pérez-Ortín JE, et al. The distribution of active RNA polymerase II along the
686 transcribed region is gene-specific and controlled by elongation factors. Nucleic
687 Acids Res. 2010;38: 4651–4664. doi:10.1093/nar/gkq215
688 36. Jordán-Pla A, Gupta I, de Miguel-Jiménez L, Steinmetz LM, Chávez S, Pelechano
689 V, et al. Chromatin-dependent regulation of RNA polymerases II and III activity

690 throughout the transcription cycle. Nucleic Acids Res. 2015;43: 787–802.
691 doi:10.1093/nar/gku1349
692 37. García-Martínez J, Delgado-Ramos L, Ayala G, Pelechano V, Medina DA, Carrasco
693 F, et al. The cellular growth rate controls overall mRNA turnover, and modulates
694 either transcription or degradation rates of particular gene regulons. Nucleic
695 Acids Res. 2016;44: 3643–3658. doi:10.1093/nar/gkv1512
696 38. Chávez S, García-Martínez J, Delgado-Ramos L, Pérez-Ortín JE. The importance
697 of controlling mRNA turnover during cell proliferation. Curr Genet. 2016;62:
698 701–710. doi:10.1007/s00294-016-0594-2
699 39. Sasidharan K, Tomita M, Aon M, Lloyd D, Murray DB. Time-Structure of the
700 Yeast Metabolism In vivo. 2012. pp. 359–379. doi:10.1007/978-1-4419-7210-
701 1_21
702 40. Klevecz RR, Bolen J, Forrest G, Murray DB. A genomewide oscillation in
703 transcription gates DNA replication and cell cycle. Proceedings of the National
704 Academy of Sciences. 2004;101: 1200–1205. doi:10.1073/pnas.0306490101
705 41. Kurniawan F, Chakraborty A, Oishi HZ, Liu M, Arif MK, Chen D, et al.
706 Phosphorylation of Orc6 During Mitosis Regulates DNA Replication and
707 Ribosome Biogenesis. Mol Cell Biol. 2024;44: 289–301.
708 doi:10.1080/10985549.2024.2356880
709 42. Girke P, Seufert W. Compositional reorganization of the nucleolus in budding
710 yeast mitosis. Mol Biol Cell. 2019;30: 591–606. doi:10.1091/mbc.E18-08-0524
711 43. Garrido-Godino AI, Gupta I, Gutiérrez-Santiago F, Martínez-Padilla AB,
712 Alekseenko A, Steinmetz LM, et al. Rpb4 and Puf3 imprint and post-
713 transcriptionally control the stability of a common set of mRNAs in yeast. RNA
714 Biol. 2021;18: 1206–1220. doi:10.1080/15476286.2020.1839229
715 44. García-Martínez J, Singh A, Medina D, Chávez S, Pérez-Ortín JE. Enhanced gene
716 regulation by cooperation between mRNA decay and gene transcription.
717 Biochim Biophys Acta Gene Regul Mech. 2023;1866.
718 doi:10.1016/j.bbagrm.2023.194910
719

720

721 # Supporting information

722 **S1 Fig. Cell cycle distribution in assessed samples.** Representative example of the
723 budding index and the FACS profile of samples in which stages in which active and total
724 RNA pol II were analysed.

725

726 **S2 Fig. Distribution of total RNA polymerase II (RNAp ChIP) and active RNA polymerase**
727 **II (GRO) at genes during the transition from G1 to G2. A**) Plot representing total RNA

728 pol II and active RNA pol II present in each gene at each time point analysed. **B**) Plot
729 representing clusters identified with SOTA.
730
731 **S3 Fig. Distribution of identified clusters within the different categories of cell cycle**
732 **genes according to their peak of maximal accumulation (CellCycle Base 3.0).** Green
733 arrows represent groups in which the enrichment or depletion of clusters is statistically
734 significant (logistic regression with BF correction).
735
736 **S4 Fig. Some periodically expressed genes exhibit dissimilar GRO and RNAp ChIP**
737 **profiles along the cell cycle. A)** Examples of G1-expressed genes (*AMS1, ARA1, CHS1,*
738 *GPD1, TPS1* and *YDL023C*) belonging to cluster D. **B)** Examples of G1- (*ALD4*, *HXT4* and
739 *HXT5*) and G1/S-expressed genes (*IDH2*, *HEM15* and *YLR327C*) from cluster F. **C)**
740 Examples of S/G2- (*ARP10*) and G2/M-expressed genes (*FKH2, STB5, TUB2, YOR246C* and
741 *YTH1)* from cluster I.
742
743 **S5 Fig. Cell cycle regulation of RiBi and RP genes.** Gene ontology analysis highlights a
744 strong enrichment of cluster A in RP and RIBI genes. Manual validation of mRNA levels
745 obtained for selected RiBi and RP genes in synchronized cells released from a G1 arrest
746 with alpha factor (10 minutes interval sampling).
747
748 **S1 Table. Experimental data.** GRO, RNAp ChIP, mRNA expression and mRNA decay data
749 for all genes, indicating the cluster where each genes is located, whether the gene has
750 been previously described as cell-cycle regulated, and whether it belongs to RiBi or RP
751 regulons. mRNA expression and decay data are from Cramer´s lab [17].

752

753 **S2 Table. Gene ontology analyses.** Results of the gene ontology analyses performed

754 with each gene cluster.

755

756

757

758

759

760

761

762

A.

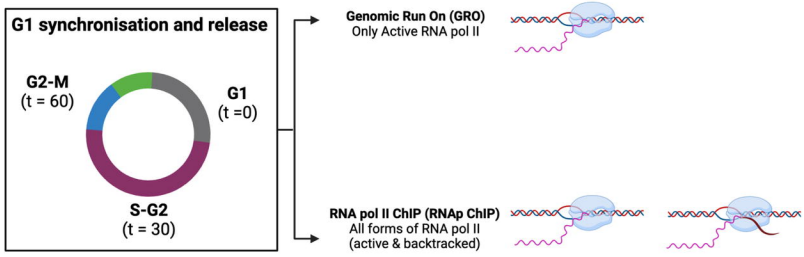
G1 synchronisation and release
G2-M
(t = 60)
G1
(t =0)
S-G2
(t = 30)
Genomic Run On (GRO)
Only Active RNA pol II
RNA pol II ChIP (RNAp ChIP)
All forms of RNA pol II
(active & backtracked)

B.

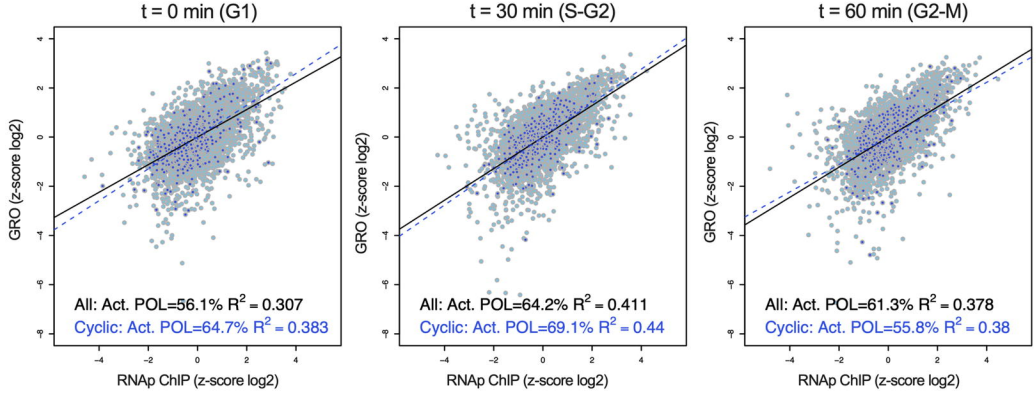
t = 0 min (G1)
t = 30 min (S-G2)
t = 60 min (G2-M)
GRO (z-score log2)
RNAp ChIP (z-score log2)
All: Act. POL=56.1% R2 = 0.307
Cyclic: Act. POL=64.7% R2 = 0.383
All: Act. POL=64.2% R2 = 0.411
Cyclic: Act. POL=69.1% R2 = 0.44
All: Act. POL=61.3% R2 = 0.378
Cyclic: Act. POL=55.8% R2 = 0.38

C.

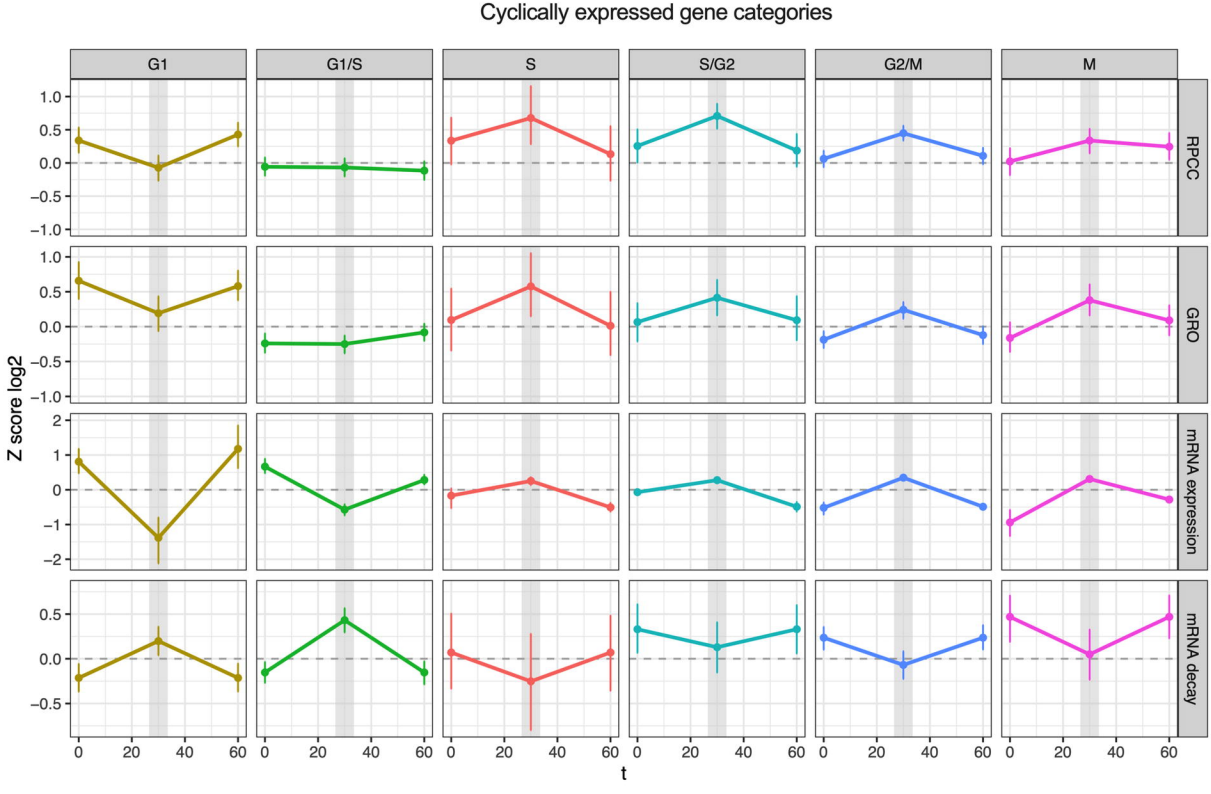
Cyclically expressed gene categories
G1
G1/S
S
S/G2
G2/M
M
RPCC
GRO
mRNA expression
mRNA decay
Z score log2
t

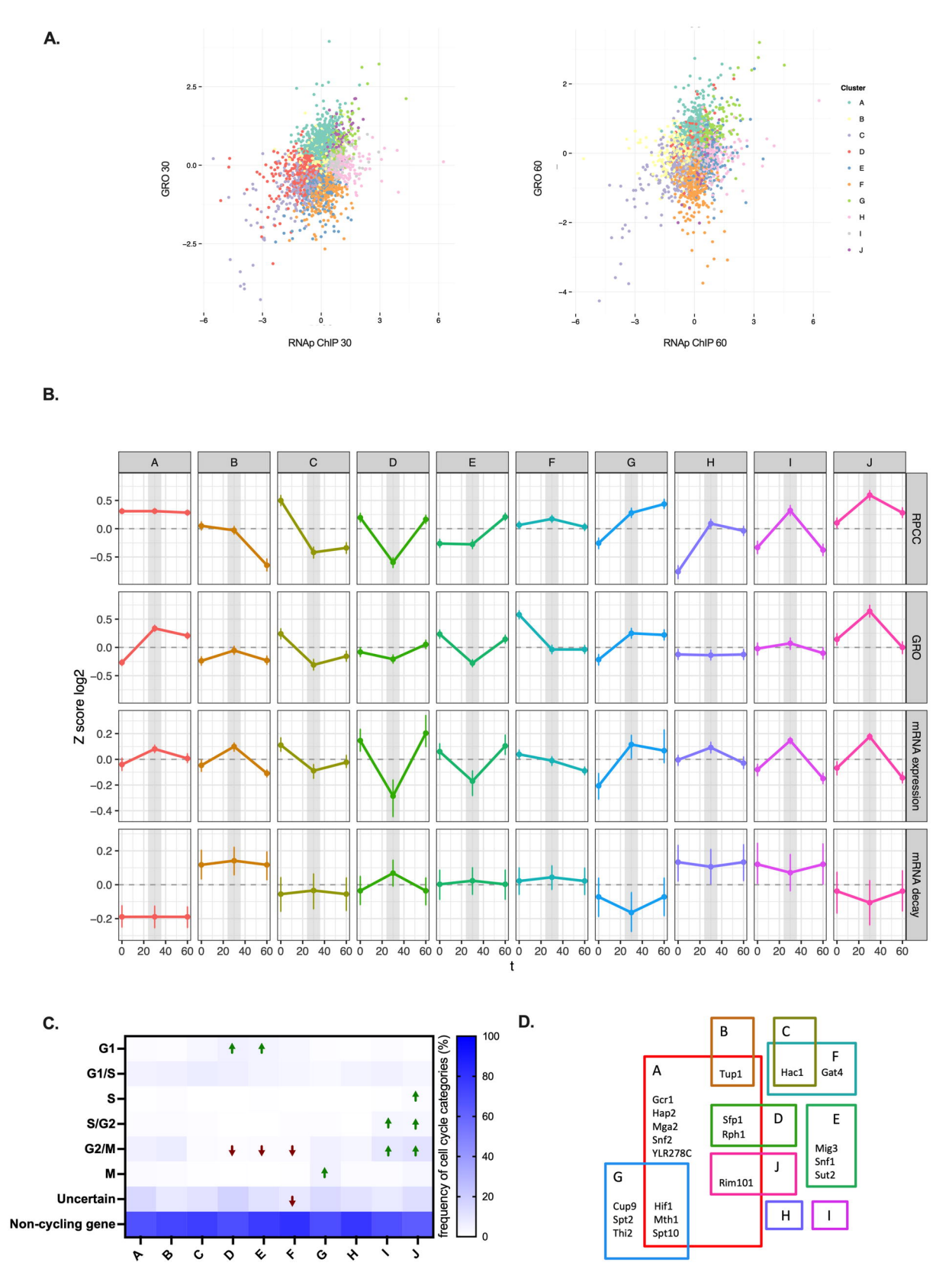
A.
GRO 30
RNAp ChIP 30
GRO 60
RNAp ChIP 60
Cluster
A
B
C
D
E
F
G
H
I
J
B.
Z score log2
RPCC
GRO
mRNA expression
mRNA decay
t
C.
G1
G1/S
S
S/G2
G2/M
M
Uncertain
Non-cycling gene
frequency of cell cycle categories (%)
D.
Tup1
Hac1
Gat4
Gcr1
Hap2
Mga2
Snf2
YLR278C
Sfp1
Rph1
Mig3
Snf1
Sut2
Rim101
Cup9
Spt2
Thi2
Hif1
Mth1
Spt10

A.

Term ID	Term Name	p_{adj} (query_1)
GO:0042254	ribosome biogenesis	3.879×10^{-34}
GO:0032991	protein-containing complex	4.802×10^{-29}
GO:0005488	binding	4.464×10^{-20}
GO:0043412	macromolecule modification	1.560×10^{-10}
GO:0003735	structural constituent of ribosome	6.916×10^{-5}
GO:0140098	catalytic activity, acting on RNA	1.510×10^{-4}
GO:0071042	nuclear polyadenylation-dependent mRNA cat...	6.064×10^{-3}
GO:0071051	polyadenylation-dependent snoRNA 3'-end pr...	6.064×10^{-3}
GO:0009156	ribonucleoside monophosphate biosynthetic pr...	6.605×10^{-3}
GO:0008170	N-methyltransferase activity	8.650×10^{-3}
GO:0004298	threonine-type endopeptidase activity	9.054×10^{-3}
GO:0043021	ribonucleoprotein complex binding	1.107×10^{-2}
GO:0051028	mRNA transport	2.655×10^{-2}
GO:0006450	regulation of translational fidelity	2.829×10^{-2}
GO:0051664	nuclear pore localization	3.334×10^{-2}
GO:0010494	cytoplasmic stress granule	4.081×10^{-2}

B.

Term ID	Term Name	p_{adj} (query_1)
GO:0016491	oxidoreductase activity	3.892×10^{-3}
GO:0016743	carboxyl- or carbamoyltransferase activity	1.291×10^{-2}
GO:0009055	electron transfer activity	4.596×10^{-2}
GO:0008652	amino acid biosynthetic process	3.904×10^{-4}
GO:0009084	glutamine family amino acid biosynthetic proce...	1.663×10^{-3}
GO:0009987	cellular process	1.006×10^{-2}
GO:0042773	ATP synthesis coupled electron transport	1.210×10^{-2}
GO:0098798	mitochondrial protein-containing complex	1.416×10^{-4}
GO:0005759	mitochondrial matrix	2.736×10^{-3}
GO:0005622	intracellular anatomical structure	5.570×10^{-3}
GO:0005750	mitochondrial respiratory chain complex III	2.516×10^{-2}
GO:0031090	organelle membrane	2.919×10^{-2}
GO:0070469	respirasome	4.943×10^{-2}

C.

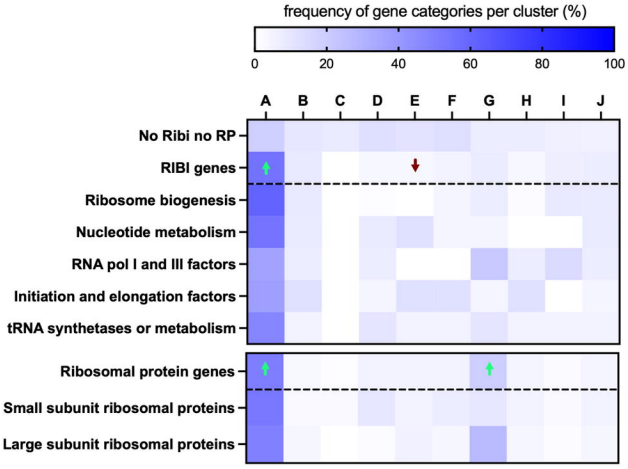

D.

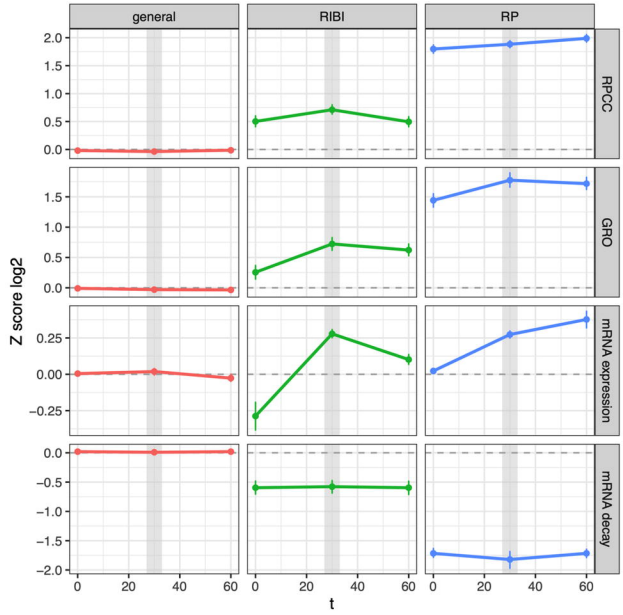
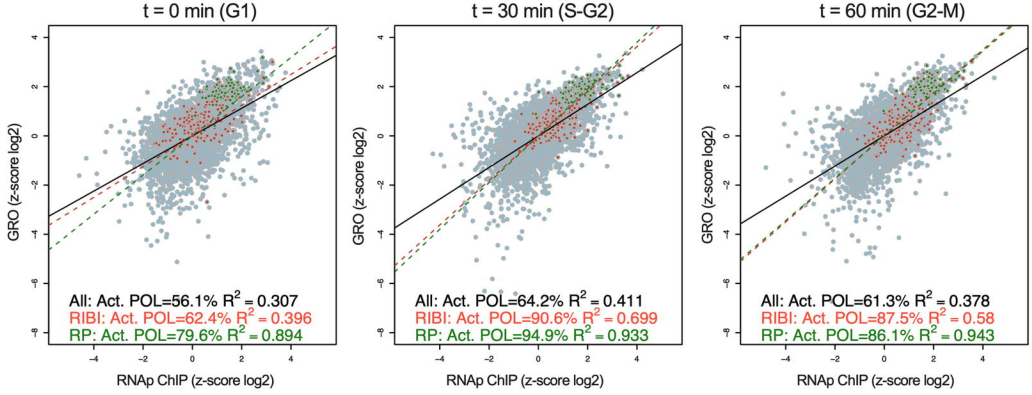
E.